STATE ESTIMATION IN UNBALANCED AC/DC NETWORKS

Marta Vanin[1,3] , Hakan Ergun[2,3], Dirk Van Hertem[2,3]*

[1]*KU Leuven, Dept. Electrical Engineering (ESAT) - Electa, Ghent, Belgium*
[2]*KU Leuven, Dept. Electrical Engineering (ESAT) - Electa, Leuven, Belgium*
[3]*Etch-EnergyVille, Thor Park 8310, Genk, Belgium*
**E-mail: marta.vanin@kuleuven.be*

Keywords: AC/DC Grids, HVDC, State Estimation

Abstract

Present HVDC links are typically point-to-point or back-to-back, such that their stationary operating state is rather straightforward to derive and incorporate in business-as-usual grid management practices. However, as HVDC connections are expected to transition towards meshed grids, e.g., in the North Sea, AC/DC state estimation is expected to become a crucial addition to the control rooms of the future, to ensure safe and reliable grid operations through real-time monitoring and application of decision support tools. This paper presents a novel, interior-point method-based unified AC/DC state estimator that is fit for future hybrid grids by enabling advanced functionalities such as the ability to capture asymmetric bipole operation.

1 Introduction

State estimation (SE) is a monitoring and diagnostic tool that has been adopted in the control room of (AC) transmission systems since the 1970s. While SE for AC/DC grids has been investigated since the 1980s [1], practical implementations are not business as usual yet, partly because of the simplicity of present point-to-point DC links, which makes them relatively straightforward to monitor. As HVDC connections are expected to evolve towards meshed grids, e.g., in the North Sea, AC/DC SE is likely to become a crucial component in the control rooms of the future.

Line commutated converters (LCC) are the oldest, conventional technology used for HVDC links. Despite the maturity of LCC, only limited work has been done on SE for LCC systems (a.o. [2, 3]), and LCC systems cannot be easily used for meshed DC grids due to difficulty in power flow reversal.

The vast majority of the AC/DC SE literature addresses the use of the more recent Voltage-Sourced Converters (VSC) [4], which are suitable for meshed operation. As the focus of our paper is on AC/DC SE solutions for off-shore wind power integration in future meshed grids, we limit the following discussion to VSC-based SE. Moreover, while we note that machine-learning methods for AC/DC SE exist [5, 6], these are still at an early research stage and are out of the scope of this paper, which discusses physics-based SE.

AC/DC SE examples in the literature either perform separate estimates for the AC and DC parts of the grid (e.g., [7, 8]), or adopt a unified approach where AC and DC states are estimated simultaneously, by collating synchronized AC, DC measurements and AC/DC network and converter models. Ayiad et al. [9] compare unified and non-unified approaches, showing that the former have better accuracy. In absence of bad data, this is generally expected: unified approaches enable a more thorough representation of the system's physics, as DC and AC states affect each other. To ensure sufficient accuracy, non-unified SE may have to resort to additional iterations to retrieve consistent states at the points of coupling between the AC and DC parts of the grid [10, 11], increasing computational time.

To obtain accurate and reliable solutions, unified AC/DC SE models should include converter equations that account for losses. To our knowledge, most literature adopts quadratic converter loss models [9, 12–14]. Sadu et al. [14] illustrate the detrimental impact of neglecting converter losses. Lambrichts et al. [15] propose a Kalman filter-based SE for AC/DC microgrids with a linear converter loss model. Thanks to their loss model and the use of phasor measurement units (PMUs), the AC/DC SE in [15] is entirely linear and thus extremely fast. However, as PMUs are presently only sparsely available in bulk power systems, SE methods are needed that rely on SCADA measurements, e.g., [16], or combinations of SCADA and PMUs, e.g. [17], and are in general nonlinear. Finally, some authors perform AC/DC SE without DC grid measurements [18]. While this may be acceptable for grids with point-to-point (or back-to-back) DC links only, incorporating DC measurements will likely be necessary in future HVDC grids.

Another feature that is receiving increasing interest in the context of future HVDC grids is the ability to operate bipoles in an asymmetric, or "unbalanced", fashion [19]. To our knowledge, there is presently limited work on the topic, and Donde al. [10] is - to date - the only AC/DC SE model expressive enough to represent unbalanced DC operation. In [10], metallic return states are incorporated to capture single-pole outages.

The main features of existing work on VSC-based AC/DC SE have been summarized in Table 1. These are compared

Note on affiliation: M. Vanin was with KU Leuven, Electa-Leuven at the time this work started.

https://doi.org/10.1049/icp.2025.1193

Table 1 Features of recent selected VSC AC/DC state estimation literature. References that would produce "duplicate" columns are not included in the table for space limits. Some compare unified and non-unified SE models. In this case, a (p) indicates their proposed/recommended method, and (b) the benchmark method.

ref. →	[9]	[12]	[8]	[20]	[21]	[15]	[10]	[16]	[22]	[18]	**This paper**
Unified	✓(p)	✓	✓(b)	✓	✓	✓	✗	✓	✓	✓	✓
Non-unified	✓(b)	✗	✓(p)	✗	✗	✗	✓	✗	✗	✗	✗
Unbalanced DC	✗	✗	✗	✗	✗	✗	✓	✗	✗	✗	✓
SCADA(-like)	✓	✓	✓	✓	✓	✗	✓	✓	✓	✓	✓
PMU	✗	✗	✓	✓	✗	✓	✗	✗	✗	✓	✓(voltage), ✗(current)
DC measurements	✓	✓	✓	✓	✓	✓	✓	✓	✓	✗	✓
Nontrivial converter loss model	✓	✓	✗	✓	✓	✓	✗	✓	✗	✗	✓

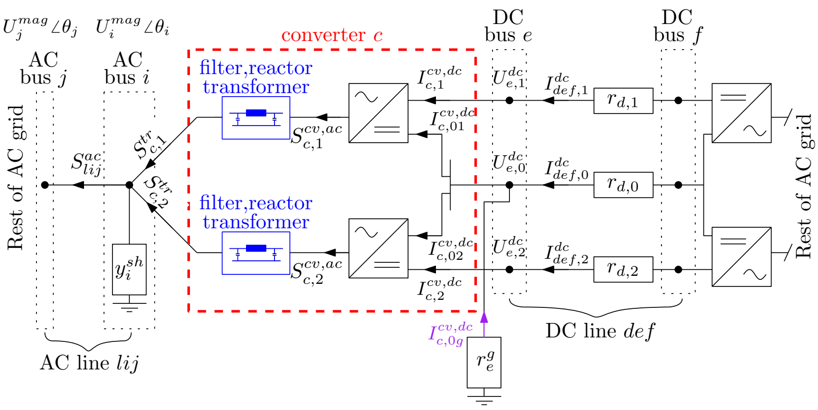

Fig. 1 Model of the AC/DC grid with all the relevant variables. The filter, reactor and transformer blocks of the converter station are omitted for conciseness. See [23] for the full mathematical description of these components.

to our implementation, which presents a unique set of features, including the support for unbalanced DC operation and DC measurements, and a quadratic representation of converter losses. *The combination of these features makes our AC/DC SE a novel and expressive implementation that is adequate to monitor future VSC AC/HVDC grids.*

2 Mathematical model

Like in [24], SE is formulated as a generic optimization problem by leveraging automatic differentiation through JUMP [25] and the IPOPT solver [26]. This approach, contrary to conventional SE implementation, enables its user to experiment with a variety of constraints and design features, and facilitates the prototyping of novel SE models that are suitable to monitor future complex AC/DC grids. Example of design choices are the residual definition, as well as the capability to capture unbalanced DC operation.

The objective of SE is to minimize the sum of residuals ρ_m, i.e., the difference between estimated system (dependent or independent) variables x_m and their measured value z_m, for all measurements m in the available set $\mathcal{M}$:

$$\text{minimize} \sum_{m \in \mathcal{M}} \rho_m, \tag{1}$$

subject to various (in)equality constraints. The **residual definition** determines the choice of the minimizer and can be easily adapted using automatic differentiation [24]. In this paper, we adopt the conventional weighted least squares:

$$\rho_m = \frac{(x_m - z_m)^2}{\sigma_m^2} \quad \forall m \in \mathcal{M}. \tag{2}$$

Additionally, the power flow equations that govern the behaviour of the whole AC/DC grid are enforced as equality constraints. All the used variables are illustrated in Fig. 1. AC-side equations in this paper are provided in polar coordinates ($U^{\text{mag}}, \angle\theta$). The implementation, however, supports voltage variables in rectangular coordinates as well.

The constraints and variables for the converter station's filter, reactor and transformer modules are omitted both from Fig. 1 and from the mathematical model in this section, for conciseness. The reader can refer to [19] for their expressions. However, note that the SE implementation does include them in their exact form, i.e., preserving their nonlinearities.

AC grid constraints:

$$\begin{aligned} P_{lij}^{ac} = g_{lij} \cdot \Big((U_i^{\text{mag}})^2 - U_i^{\text{mag}} U_j^{\text{mag}} \cdot \cos(\theta_i - \theta_j) \Big) \\ - b_{lij} \cdot U_i^{\text{mag}} U_j^{\text{mag}} \cdot \sin(\theta_i - \theta_j) \;\; \forall lij \in \mathcal{T}^{ac} \end{aligned} \tag{3}$$

$$\begin{aligned} Q_{lij}^{ac} = -b_{lij} \cdot \Big((U_i^{\text{mag}})^2 - U_i^{\text{mag}} U_j^{\text{mag}} \cdot \cos(\theta_i - \theta_j) \Big) \\ - g_{lij} \cdot U_i^{\text{mag}} U_j^{\text{mag}} \cdot \sin(\theta_i - \theta_j) \;\; \forall lij \in \mathcal{T}^{ac} \end{aligned} \tag{4}$$

$$\sum_{lij\in\mathcal{T}^{ac}} S^{ac}_{lij} + \sum_{mi\in\mathcal{T}^{load,ac}} S^{mi} - \sum_{ti\in\mathcal{T}^{tr,ac}} \sum_{\phi\in\{1,2\}} S^{ti}_{\phi} = \sum_{gi\in\mathcal{T}^{gen,ac}} S^{gi} + y_i^{shunt}(U_i^{\text{mag}})^2 \;\; \forall i \in \mathcal{I} \quad (5)$$

Eq. (3)-(4) represent active and reactive power flows through all AC lines/topologies $\mathcal{T}^{ac}$. Apparent powers are defined as $S = P + im\cdot Q$ with $im := \sqrt{-1}$. Eq. (5) represents the power balance at any AC node i, where $\mathcal{T}^{load,ac}, \mathcal{T}^{tr,ac}, \mathcal{T}^{gi,ac}$ are the sets of loads, transformer terminals and generators connected to node i (such sets may be empty if no components are present). Note (see Fig. 1) that the transformers in (5) are, specifically, those that are part of the converter substation[1]. As such, as the operation of DC links and converter may explicitly be unbalanced, the transformer contribution is written as the sum of the power in the positive and negative terminals. Subscripts ϕ indicate the DC terminals, where 0, 1 and 2 are, respectively, the neutral, positive and negative conductor.

y_i^{shunt} is the impedance of possible shunt components that may be connected to i.

DC grid constraints: The rectangular current-voltage formulation is used for the DC power flow equations, as the presence of a return conductor with potentially (near-)zero voltage makes other formulations unsuitable [27]. The Ohm's law for any DC line d depends on each conductor's resistance $r_{d,\phi}$:

$$I^{dc}_{def} = (1/r_{d,\phi})\cdot(U^{\text{dc}}_{e,\phi} - U^{\text{dc}}_{f,\phi}) \;\; \forall def \in \mathcal{T}^{dc}, \phi\in\{0,1,2\} \quad (6)$$

The current injections from all converters c placed between an AC node and DC node e are equal to the power flows through all DC lines that start from node e, s.t.:

$$\sum_{cie\in\mathcal{T}^{\text{cv}}} I^{cv,dc}_{c,\phi} + \sum_{def\in\mathcal{T}^{dc}} I^{dc}_{def,\phi} = 0 \;\; \forall e\in\mathcal{E}, \phi\in\{1,2\} \quad (7)$$

where $\mathcal{E}$ is the set of all DC nodes. Neutral conductor $\phi = 0$ grounding is supported, thus:

$$\sum_{cie\in\mathcal{T}^{\text{cv}}} I^{cv,dc}_{c,0} + \sum_{def\in\mathcal{T}^{dc}} I^{dc}_{def,0} + \sum_{cie\in\mathcal{T}^{\text{cv}}} I^{cv,dc}_{c,0g} = 0 \;\; \forall e\in\mathcal{E}, \quad (8)$$

where the ground current depends on grounding resistance r^g_e:

$$I^{\text{cv, dc}}_{c,0g} = U^{\text{dc}}_{e,0}/r^g_e. \quad (9)$$

AC/DC converter constraints: The apparent power $S^{\text{cv, ac}}$ on the AC side of converter c is defined through its AC voltages and currents, with $(\cdot)^*$ indicating the complex conjugate:

$$S^{\text{cv, ac}}_{c,\phi} = U^{\text{cv}}_{c,\phi}(I^{\text{cv}}_{c,\phi})^* \;\; \forall c\in\mathcal{C}, \phi\in\{1,2\}. \quad (10)$$

The AC current magnitude $I^{\text{cv, mag}}_{c,\phi} = |I^{\text{cv}}_{c,\phi}|$ is generally used to model the converter power losses. Here, we use the quadratic loss model from [23]:

$$P^{\text{cv, loss}}_{c,\phi} = a^{\text{cv}}_{c,\phi} + b^{\text{cv}}_{c,\phi}\cdot I^{\text{cv, mag}}_{c,\phi} + c^{\text{cv}}_{c,\phi}(I^{\text{cv, mag}}_{c,\phi})^2 \;\; \forall c\in\mathcal{C}, \phi\in\{1,2\}, \quad (11)$$

the values of coefficients $a^{\text{cv}}_{c,\phi}, b^{\text{cv}}_{c,\phi}, c^{\text{cv}}_{c,\phi}$ is as in [23].

Given the losses, the converter power balance reads as:

$$P^{\text{cv, loss}}_{c,\phi} = P^{\text{cv, ac}}_{c,\phi} + I^{\text{cv, dc}}_{c,\phi}\cdot U^{\text{dc}}_{e,\phi} + I^{\text{cv, dc}}_{c,\phi 0}\cdot U^{\text{dc}}_{e,0} \;\; \forall c\in\mathcal{C}, \phi\in\{1,2\}. \quad (12)$$

Kirchhoff's current law completes the converter model:

$$I^{\text{cv, dc}}_{c,\phi} + I^{\text{cv, dc}}_{c,\phi 0} = 0 \;\; \forall c\in\mathcal{C}, \phi\in\{1,2\}, \quad (13)$$

$$I^{\text{cv, dc}}_{c,0} + \sum_{\phi\in\{1,2\}} I^{\text{cv, dc}}_{c,\phi 0} = 0 \;\; \forall c\in\mathcal{C}. \quad (14)$$

Finally, thanks to the use of an interior-point solver, inequality constraints and variable bounds can be added to the SE problem. We use this property to enforce system knowledge by, e.g., setting minimum voltage magnitudes to 0.2 p.u. With respect to an optimal power flow model, the SE bounds need to be chosen more carefully, as non-nominal operating conditions may occur and need to be detected by the SE, i.e., the bounds should not exclude optimal solutions from the search space.

3 Numerical results

For the numerical experiments in this paper, we assume that all measurements $m \in \mathcal{M}$ are part of the power flow formulation's variable space χ, i.e., all z_m in (1) directly measure a $x_m \in \chi = \{U^{\text{mag}}, \theta, P, Q\}$. When additional measurements are added, e.g., current magnitudes, that are not part of the chosen formulation's space, extra "mapping constraints" need to be added, as described in [24]. While these constraints are straightforward to add through our automatic differentiation-based SE, here they are omitted for simplicity, such that the the AC/DC SE is fully described by (1)-(14).

Table 2 reports the per unit voltage value for each conductor of the DC buses of the CASE5_2GRIDS_MC test network used for the numerical analysis in [19]. The network has 11 AC buses, 4 DC buses and 3 converters. Because a monopolar link is connected to the negative and neutral conductors of the bipolar links stemming from converter #1 and #2 (see Fig. 8 in [19]), the poles are not symmetrical.

The "True U^{dc}" states in the table are the results of power flow calculations using the network's load data. Synthetic measurements are built from the power flow results to be used as input for AC/DC SE calculations, which is standard practice in the literature. The "noiseless SE result" in the table reveal that if no noise is added to the true states, the magnitudes calculated by the SE are the same as the "True U^{dc}, which validates the SE model and implementation [24]. Furthermore, the non-zero values for the return conductor columns $\phi = 0$ show that the SE effectively captures DC unbalance operations.

For the noisy measurement case, we assume zero-mean Gaussian noise for all measurements. The measurement set consists of active and reactive power flows at all AC branches (measured at both ends of the lines), active and reactive power injections from all loads and generators, voltage magnitudes at all buses, and voltage angles at all AC buses, mimicking a combination of SCADA and PMU measurements. The 3σ values are 0.5% for AC voltages, 1% for generation and DC voltages, 2% for demand, and 1.5% for AC power flows. The percentage

[1] *"Regular" transformers are characterized by the same equations and are supported in our SE. For these, the terminal distinction is not necessary.*

Table 2 AC/DC SE results (voltage magnitudes) for the DC buses of network CASE5_2GRIDS_MC, in per unit.

	True U^{dc}			Noiseless SE result			Noisy SE result		
	$\phi=1$	$\phi=2$	$\phi=0$	$\phi=1$	$\phi=2$	$\phi=0$	$\phi=1$	$\phi=2$	$\phi=0$
DC bus #1	1.09022	-1.08012	-0.01009	1.09022	-1.08012	-0.01009	1.08911	-1.07971	-0.01077
DC bus #2	1.10000	-1.10000	1e-17	1.10000	-1.10000	5e-14	1.09863	-1.10000	2e-11
DC bus #3	1.08043	-1.08120	0.00077	1.08043	-1.08120	0.00077	1.07960	-1.08021	-0.00076
DC bus #4	1.00000	-1.05916	-0.03105	1.00000	-1.05916	-0.03105	1.00009	-1.05892	-0.03156

Table 3 Summary of AC/DC SE results for CASE39_MCDC and CASE67_MCDC, with noise. All values are in per unit and refer to absolute voltage magnitude differences with respect to the ground truth values. MAE stands for mean absolute error.

	MAE DC buses	Max. err. DC buses	MAE AC buses	Max. err. AC buses	solve time [s]
CASE39_MCDC	1.2e-3	6.4e-3	2.2e-4	5.2e-4	0.7
CASE67_MCDC	8.6e-4	6.8e-3	1.0e-4	4.1e-4	1.5

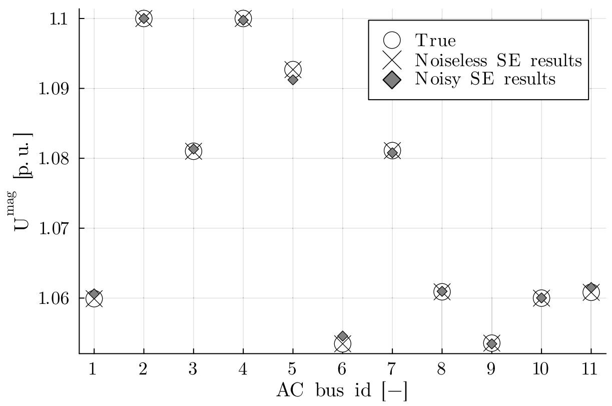

Fig. 2. AC Voltage magnitudes, CASE5_2GRIDS_MC.

refers to the measurement value. The "noisy SE result" column in Table 2 shows that the SE calculations are still accurate in the presence of noise.

Fig. 2 reports the voltage estimates of the network's AC buses, which confirm the SE quality and conclusions.

SE calculations are repeated for the larger CASE39_MCDC and CASE67_MCDC networks from [19], whose results are summarized in Table 3, as illustrations are omitted due to page limits. The calculations are performed on an HP EliteBook 865 with 16GB RAM and AMD Ryzen 7 PRO 6850U processor with JULIA 1.11 and IPOPT 3.14.17 with MUMPS 5.7.3. The solve times appear acceptable for the purposes of this SE, which does not aim to be the final estimator to deploy in real-time, but a platform to facilitate prototyping SE models that are suitable for complex AC/DC grids, similarly to what [24] describes for distribution systems SE.

4 Conclusion

This paper presents a unified AC/DC state estimation implementation that relies on automatic differentiation and supports unbalanced DC grids. Through automatic differentiation, it is possible to customize the state estimator and incorporate novel features and constraints that are necessary to adequately monitor the complex future AC/DC grids. The developed SE allows to capture asymmetric operation of bipolar HVDC connections and their non-zero neutral voltages. Future work will extend on the presented implementation to incorporate, among other, additional power flow formulations, measurement functions and states, to enable the development of state estimators that further improve on the state of the art.

5 Acknowledgements

This work has been funded through the Horizon Europe project DC Protection, Security, Control and Optimisation (PROS-ECCO) - Grant Agreement: 101160687 - which the authors would like to acknowledge.

6 References

[1] H. Sirisena and E. Brown, "Inclusion of hvdc links in ac power-system state estimation," *IEE Proc. C-Generat., Transmiss. Distrib.*, vol. 128, no. 3, pp. 147–154, 1981.

[2] O. Darmis, G. Karvelis, and G. Korres, "Pmu-based state estimation for networks containing lcc-hvdc links," *IEEE Trans. Power Syst.*, vol. 37, no. 3, pp. 2475–2478, 2022.

[3] W. Li and L. Vanfretti, "A pmu-based state estimator considering classic hvdc links under different control modes," *Sustainable Energy, Grids and Networks*, vol. 2, pp. 69–82, 2015.

[4] G. Karvelis, G. Korres, and O. Darmis, "State estimation using scada and pmu measurements for networks containing classic hvdc links," *Electr. Power Syst. Res*, vol. 212, p. 108544, 2022.

[5] M. Huang, Z. Wei, and Y. Lin, "Forecasting-aided state estimation based on deep learning for hybrid ac/dc distribution systems," *Appl. Energy*, vol. 306, p. 118119, 2022.

[6] M. Huang, J. Zhao, and Z. Wei, et al., "Decentralized robust state estimation for hybrid ac/dc distribution systems with smart meters," *INT. J. ELEC. POWER*, vol. 136, p. 107656, 2022.

[7] W. Feng, Q. Shi, and H. Cui, et al., "Using lagrangian relaxation to include operating limits of vsc-mtdc system for state estimation," in *IEEE PES General Meeting*, 2020, pp. 1–5.

[8] Kong, et al., "Three-stage distributed state estimation for ac-dc hybrid distribution network under mixed measurement environment," *IEEE Access*, vol. 6, pp. 39 027–39 036, 2018.

[9] M. Ayiad, H. Leite, and H. Martins, "State estimation for hybrid vsc based hvdc/ac transmission networks," *Energies*, vol. 13, no. 18, 2020.

[10] V. Donde, X. Feng, I. Segerqvist, and M. Callavik, "Distributed state estimation of hybrid ac/hvdc grids by network decomposition," *IEEE Trans. Smart Grid*, vol. 7, no. 2, pp. 974–981, 2016.

[11] N. Xia, H. B. Gooi, S. Chen, and W. Hu, "Decentralized state estimation for hybrid ac/dc microgrids," *IEEE Systems Journal*, vol. 12, no. 1, pp. 434–443, 2018.

[12] M. Ayiad, H. Leite, and H. Martins, "State estimation for hybrid vsc based hvdc/ac: Unified bad data detection integrated with gaussian mixture model," *IEEE Access*, vol. 9, pp. 91 730–91 740, 2021.

[13] M. Pau, A. Sadu, and S. Pillai, et al., "A state estimation algorithm for hybrid ac/dc networks with multi-terminal dc grid," in *IEEE PES Innovative Smart Grid Technologies Conf. Europe*, 2016, pp. 1–6.

[14] S. P. F. P. A. Sadu, M. Pau and A. Monti, "Impact of uncertainty propagation on the design of state estimation for hybrid ac-dc grids," in *IEEE Int. Workshop on Applied Measurements for Power Systems*, 2016, pp. 1–6.

[15] W. Lambrichts and M. Paolone, "Linear recursive state estimation of hybrid and unbalanced ac/dc micro-grids using synchronized measurements," *IEEE Trans. Smart Grid*, vol. 14, no. 1, pp. 54–67, 2023.

[16] A. de la Villa Jaen, E. Acha, and A. G. Exposito, "Voltage source converter modeling for power system state estimation: Statcom and vsc-hvdc," *IEEE Trans. Power Syst.*, vol. 23, no. 4, pp. 1552–1559, 2008.

[17] G. Pontus, "Centralized versus distributed state estimation for hybrid ac/hvdc grid," in *IEEE PES Innovative Smart Grid Technologies Conf. Europe*, 2017, pp. 1–6.

[18] E. Zamora-Cárdenas, C. Fuerte-Esquivel, and A. Pizano-Martínez, et al., "Hybrid state estimator considering scada and synchronized phasor measurements in vsc-hvdc transmission links," *Electr. Power Syst. Res.*, vol. 133, pp. 42–50, 2016.

[19] C. K. Jat, J. Dave, D. Van Hertem, and H. Ergun, "Hybrid ac/dc opf model for unbalanced operation of bipolar hvdc grids," *IEEE Trans. Power Syst.*, pp. 1–11, 2023.

[20] R. Martínez-Parrales and C. Fuerte-Esquivel, "A new unified approach for the state estimation and bad data analysis of electric power transmission systems with multi-terminal vsc-based hvdc networks," *Electr. Power Syst. Res.*, vol. 160, pp. 251–260, 2018.

[21] Z. Fang, Y. Lin, and S. Song, et al., "A comprehensive framework for robust ac/dc grid state estimation against measurement and control input errors," *IEEE Trans. Power Syst.*, vol. 37, no. 2, pp. 1067–1077, 2022.

[22] A. Mouco and A. Abur, "A robust state estimator for power systems with hvdc components," in *North American Power Symp.*, 2017, pp. 1–5.

[23] H. Ergun, J. Dave, D. Van Hertem, and F. Geth, "Optimal power flow for ac–dc grids: Formulation, convex relaxation, linear approximation, and implementation," *IEEE Trans. Power Syst.*, vol. 34, no. 4, pp. 2980–2990, 2019.

[24] M. Vanin, T. Van Acker, R. D'hulst, and D. Van Hertem, "A framework for constrained static state estimation in unbalanced distribution networks," *IEEE Trans. Power Syst.*, vol. 37, no. 3, pp. 2075–2085, 2022.

[25] I. Dunning, J. Huchette, and M. Lubin, "JuMP: A modeling language for mathematical optimization," *SIAM Rev.*, vol. 59, no. 2, pp. 295–320, 2017.

[26] A. Wächter and L. Biegler, "On the implementation of an interior-point filter line-search algorithm for large-scale nonlinear programming," *Math. Program.*, vol. 106, no. 1, pp. 25–57, 2006.

[27] F. Geth, "Pitfalls of zero voltage values in optimal power flow problems," *IEEE PES General Meeting*, 2023.